



Study on the Freeze-Thaw Damage of Granite Under Impact Loading

Yinghua Huang · Xuli Liang  · Lei Wen · Jiangfang Chang

Received: 30 July 2018 / Accepted: 27 September 2019 / Published online: 11 October 2019
© Springer Nature Switzerland AG 2019

Abstract The freeze-thaw damage of granite was studied used SHPB tests and numerical simulation in the paper. All the granite samples were taken from high altitude localities in Tibet, China, which were made impact loading test after freeze-thaw cycles. The strain rate was unified in the use of SHPB tests combined with numerical simulation to analyze the relationship between dynamic strength and freeze-thaw cycles. The results shows, under different freeze-thaw cycles, the shapes of the reflected and transmitted waves before and after freeze-thaw are different, mainly reflected in the great difference of the curves before and after the peak. With the increase of the freeze-thaw cycles, the peak value of the strength curves decrease apparently and the peak stress decreases apparently after 10 cycles. Samples have different strain rates with the same incident wave under different freeze-thaw cycles. The dynamic

strength of granite is associated with the strain rate and the freeze-thaw cycles. Study on the freeze-thaw damage of granite under impact loading is the basis of the granite dynamic constitutive relation and it is important to analyze the stability of open-pit mine slope in seasonal frozen regions.

Keywords Freeze-thaw cycles · Numerical simulation · SHPB test · Dynamic strength · Rock

1 Introduction

The rock failure due to freeze-thaw weathering occurs mainly in the environments where temperatures frequently fluctuate above and below freezing point (Yavuz et al. 2006). The physical and mechanical properties of rock change after different freeze-thaw cycles. When water turns into ice, it increases in volume by up to 9%, thus giving rise to an increase in the pressure within the pores (Bell 2000). The volume expansion due to phase change between water and ice during the freeze process could result in the extension of micro crack. In addition, the uneven contraction and expansion of the different mineral compositions of rock is one of the important causes for freeze-thaw damage.

The effects of freeze-thaw cycles on the physical and mechanical properties of rocks have been studied

Y. Huang
Changsha Institute of Mining Research Co. Ltd, Lushan
South Road 343, Changsha City, China

X. Liang (✉)
School of Exploration Technology and Engineering,
Hebei GEO University, Huaian East Road 136,
Shijiazhuang City, China
e-mail: liangxuli@foxmail.com

L. Wen · J. Chang
Department of Engineering Mechanics, Shijiazhuang
Tiedao University, Beierhuan East Road 17,
Shijiazhuang City, China

by researchers in different ways. Celik (2017) studied water absorption and P-wave velocity of travertine rocks during freeze-thaw weathering process. Sondergl and Rai (2007) studied the change rule of the compression coefficient and resistance coefficient of the sandstone due to the freeze-thaw cycles. Ince and Fener (2016) determined the deteriorated pyroclastic rock's index mechanical properties and developed a statistical model for estimating percentage loss of uniaxial compressive strength. Hashemi et al. (2018) investigated the performance of the Schmidt hammer test in the durability assessment of carbonate building stones against frost weathering. Wang Liping et al. (2019) studied the physical parameters and the triaxial compression mechanical characteristics of fine sandstone and coarse sandstone subjected to different freeze-thaw cycles. Ghobadi et al. 2016 predicted the long-term durability of tuffs against freeze-thaw using a decay function. Walbert et al. (2015) tested and analyzed the physico-mechanical properties of three French limestones during the freeze-thaw cycles. Graham and Au 1985 investigated softening of natural clay by freezing-thawing. Saad et al. 2010 determined the influence of water flows into porous network on frost weathering of rocks. Mutluturk et al. 2004 proposed a decay function model for the integrity loss of rock under freeze-thaw cycles. Altindag et al. (2004) and Amin et al. (2013) supplied and verified the decay function model again. Huang et al. (2018) established a damage constitutive model under freeze-thaw and evaluated the stability of rock engineering in cold regions. Khuda et al. (2017) investigated the effect of freeze-thaw cycles on the flexural strength of granite panels. The CT scan and nuclear magnetic resonance are also used in the study of the rock freeze-thaw damage (Li et al. 2016; Liu et al. 2016). In general, studies on the physical and mechanical properties of rock and the failure mechanism of rock under freeze-thaw cycles are the main aspects in this area. Nowadays, researches mainly focus on the static mechanical properties in this area, however, there are very few researches on the dynamic strength of the rock under freeze-thaw cycles.

The split Hopkinson pressure bar (SHPB) technique is one of the primary experimental methods used to evaluate the dynamic-mechanical properties of rock (Anderson and O'donoghue 1992; Bailly et al. 2011). Using the same impact velocity in SHPB test, the strain rates of rock samples are different under

different freeze-thaw cycles, so it is hard to obtain the dynamic characteristic of rock with the same strain rate under the freeze-thaw cycles. It is an effective method to obtain large number data utilizing LS-DYNA finite element software, which has been recognized as one of the best computer software for simulating the dynamic behavior (Yu et al.2010). The detailed and abundant data could be obtained through simulating the process of SHPB test. The HJC constitutive model (Holmquist et al. 1993) can be used to describe the mechanical behavior of rock under high-speed impact. At present, some researchers have carried out a serious of studies on the selections of the parameters of the HJC model (Wu et al. 2011; Christopher 2011; Polanco-Loria et al. 2008). Many researchers have verified the reliability of the HJC model (Christopher 2011; Khoogar et al. 2013; Liu et al.2012). The SHPB tests could be complementary with the numerical simulation to study the dynamic strength of rock under freeze-thaw cycles.

The statistics shows that the area of permafrost, seasonal permafrost and instantaneous permafrost on the earth accounts for almost 50% of the land area, mainly distributed in Russia, Canada, China, Alaska of United States, northern Europe and other places. In China, Area of permafrost regions and seasonal regions is 21.5% and 53.5% respectively, that is there is almost 75% of the land area changes periodically from winter to summer, and its total area of cold area ranks third in the world (Xu 2006). A large number of rock engineering projects are more or less affected by freeze-thaw damage, such as Yulong copper mine and Zhibula copper mine which are located in Tibet, high altitude areas, where the stability of rock slopes are easily affected by freeze-thaw.

the open-pit mining slope in such cold region would resist dynamic load such as blasting load, so it is useful to make research on the change law of the rock dynamic strength under freeze-thaw cycles. In this paper, on the basis of the change law of the dynamic strength of granite under freeze-thaw cycles were obtained according to the results of dynamic tests and numerical simulations.

2 Test Method and Results

2.1 Test Method

The granite were drilled from an open-pit mine in Tibet. The diameter of the rock core is about 50 mm. All the samples are made into cylinders with the diameter of 50 mm, while the heights for the uniaxial compressive strength test, tensile strength test and SHPB test are 100 mm, 35 mm, and 30 mm respectively. All the samples are selected using P-wave velocity tester. The samples for the different kinds of tests are divided into four groups, and each group had three samples. The temperature varies from -20 to 20 °C, and the maximum freeze-thaw cycles is 60. Physical–mechanical properties of the granite samples are tested every 20 cycles. The main instruments are: cryogenic box, rock P-wave velocity tester, electrothermal blowing dry box, electronic scales, specimen saturation equipment and 200 tons electrohydraulic servo controlled rock pressure testing machine, split Hopkinson pressure bar (SHPB). The cryogenic box is used for freeze thaw cycle test, and the freeze time is 12 h, the thawing time is 12 h, total 24 h; the rock P-wave velocity tester is used for measuring the longitudinal wave velocity of the samples to help select samples; the electrothermal blowing dry box is used for drying the samples; the electronic scales is used for weighing the samples to calculate the density; the specimen saturation equipment is used for specimen saturation, and the vacuum pressure value is 0.1 MPa, the extraction time is 6 h and the soaking time is 24 h; 200 tons electrohydraulic servo controlled rock pressure testing machine is used for testing the static mechanical properties of the samples; the SHPB testing system is used for testing dynamic mechanical properties of the samples.

The input bar, output bar and absorption bar of the SHPB testing system are made by high strength nickel alloy steel (ultimate strength is 800 MPa, wave velocity is 5400 m/s, density is 7810 kg/m^3). The lengths of the input bar, output bar and absorption bar are 3000 mm, 2000 mm, and 500 mm, respectively. All the bars are 50 mm in diameter. The testing procedures of freeze-thaw cycles obey the “Specifications for rock tests in water conservancy and hydroelectric engineering (SL264-2001) (Yangtze River Scientific Research Institute 2001)”. The quality and dimension of rock samples are measured every 20

freeze and thaw cycles to obtain the density. Three set of samples are taken out for uniaxial compressive, tensile and SHPB test respectively, in order to obtain the samples’s uniaxial compressive strength, tensile strength, elasticity modulus, poisson’s ratio and the forms of reflected wave and transmitted wave under the dynamic load. The tensile strength of the samples are obtained by split method. The uniaxial compressive strength, elasticity modulus, poisson ratio are obtained utilizing the rock pressure testing system. In the uniaxial compression tests, the samples are loaded at the rate of 0.5 Mpa/s until the failure. Poisson’s ratios are measured by extensometer.

The dynamic stress–strain curves of granite are obtained utilizing SHPB (shown in Fig. 1).

2.2 Test Results

The physical and static parameters of granite under the freeze-thaw cycles are obtained through tests, shown in Table 1. The typical static stress–strain curves of granite obtained through uniaxial compression test are shown in Fig. 2. The shape of incident wave, reflected wave and transmitted wave under different freeze-thaw cycles (0 cycle, 20 cycles, 40 cycles and 60 cycles) obtained using SHPB are shown in Fig. 3. The photographs of the typical damage samples in the SHPB tests are shown in Fig. 4.

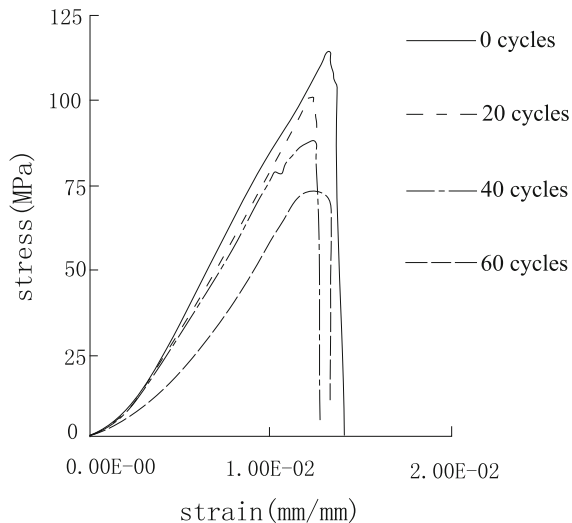
The density of the granite decreases with the increase of the freeze-thaw cycles, and the changing rate of density is -0.2% when the freeze-thaw cycles is 60. The shapes of the stress–strain curves are similar under different freeze-thaw cycles, which show the characteristics of brittle failure. The initial compaction stage of the stress–strain curves become longer obviously with the increase of the freeze-thaw cycles, which proves the freeze-thaw cycles could result in the development of the inner micro cracks.



Fig. 1 Split Hopkinson pressure bar

Table 1 Physical and statics parameters of granite under different freeze-thaw cycles

Freeze-thaw cycles	0	20	40	60
Density/kg/m ³	2727.5	2725.4	2722.3	2721.9
Uniaxial compressive strength/MPa	117.2	106.7	84.5	72.0
Tensile strength/MPa	8.77	7.56	5.84	5.22
Elastic modulus/GPa	25.52	18.05	13.58	10.15
Poisson's ratio	0.257	0.262	0.267	0.265

**Fig. 2** Typical stress–strain curves of granite

The uniaxial compressive strength, tensile strength and elastic modulus of the samples decrease obviously with the increase of the freeze-thaw cycles.

Under the dynamic load, the rock cracks paralleled to the axis of the sample could be formed. The samples are in the transverse tensile failure mode. The damage degree of the samples is larger with the increase of the freeze-thaw cycles, and more fragments could be formed in the SHPB test. The shapes of the incident wave are the same because of the same bullet's initial speed in the SHPB test, but the shapes of the reflected and transmitted wave change obviously with the increase of the freeze-thaw cycles. The shape of the incident wave is the standard half-sine wave, while the shape of the reflected wave and the transmitted wave are irregular, which are associated with the damage of the samples.

3 HJC Constitutive Model and Numerical Simulations

Because the strain rates of samples under the same incident wave are different for different freeze-thaw cycles in SHPB test, therefore, it is hard to obtain the dynamic strength data of granite with the same strain rate under different freeze-thaw cycles only rely on the laboratory tests. It is necessary to supply additional large number data using numerical simulation method.

3.1 Finite Element Model and the Selection of the Incident Wave

The element model used ANSYS software (version12.0) was set up. The partial enlargement of the element model is shown in Fig. 5.

The calculation model was established based on the symmetry of the structure. The model is meshed used eight nodes hexahedron element. For the numerical simulation of samples under different freeze thaw cycles, appropriate calculation time is defined to end the calculation. The automatic-surface-to-surface contact algorithm is used between the bar and sample. When the parameters of the samples are defined the same with the bar, the parameters of the contact surface are adjusted so that there is basically no reflected wave in the input bar, that is the suitable parameters. No restriction is made on the end of the transmission bar, because the stress wave of the sample has undergone multiple reflections before the arrival of Terminal reflected wave, which satisfies the assumption of stress uniformity, and the influence of the reflected wave at the end of the transmission bar can be ignored.

According to the research conclusions (Dong 2005), in SHPB numerical simulation, if the mesh size is less than 1.5 cm, the accuracy of simulation is very little improved by decreasing the mesh size,

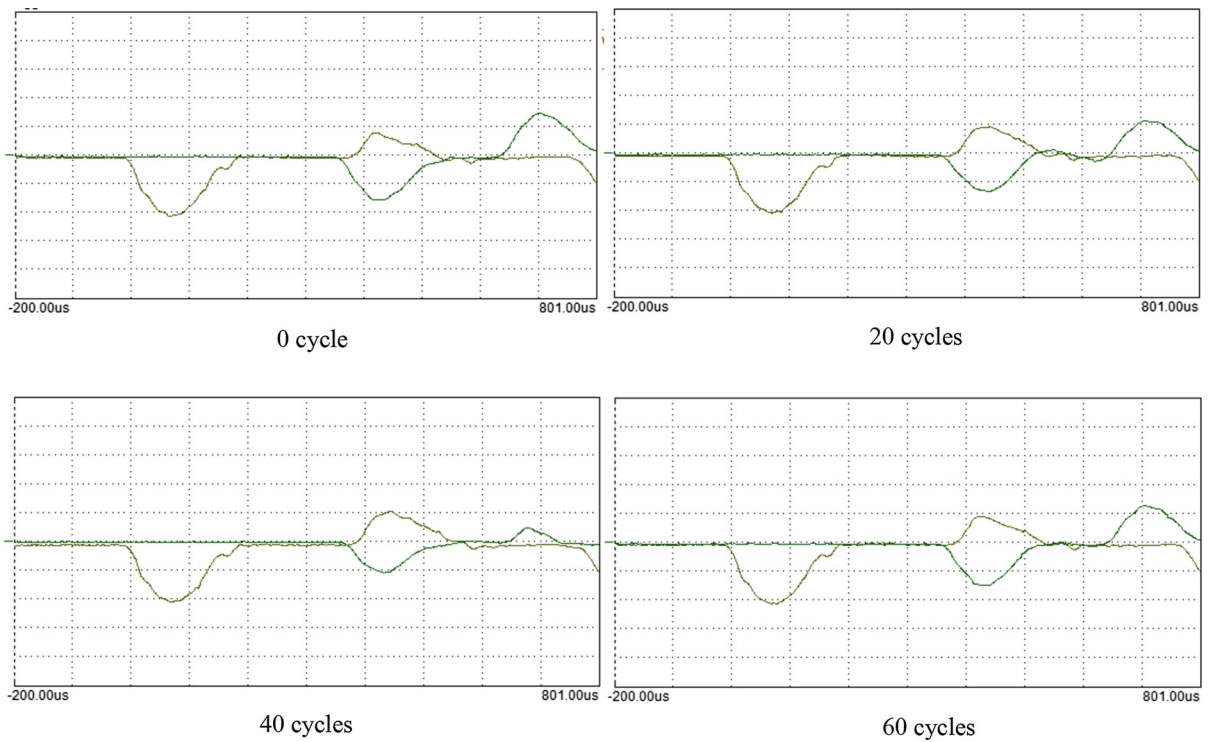


Fig. 3 Incident wave, reflected wave and transmitted wave in SHPB tests

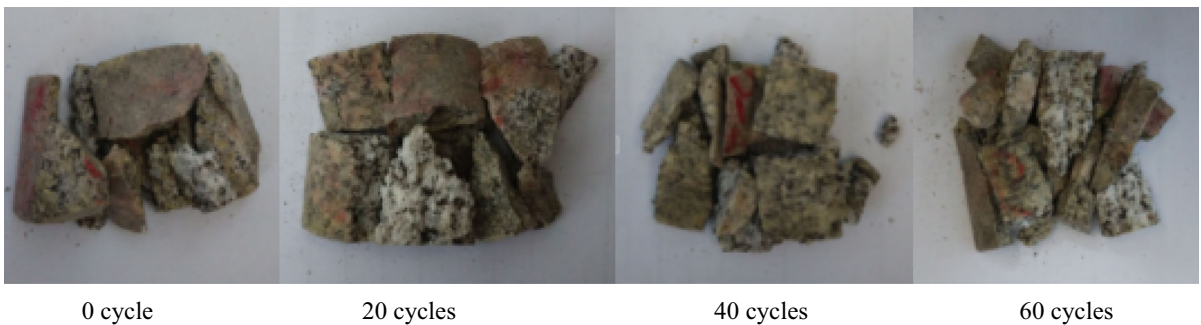


Fig. 4 Photographs of the typical damage samples in SHPB tests

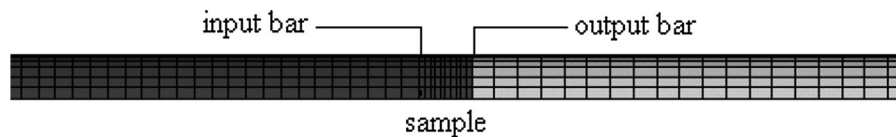


Fig. 5 Partial enlargement of the element model

therefore, the mesh size is both 1.5 cm for input bar and transmission bar, and the mesh is locally refined.

The half-sine stress wave is imposed directly on the end surface of the input bar. the mathematical expression of the half-sine wave is:

$$P(t) = \begin{cases} P_{\max} \left[\frac{1}{2} - \frac{1}{2} \cos(2\pi\omega t) \right] & (t < 1/\omega) \\ 0 & (t \geq 1/\omega) \end{cases} \quad (1)$$

where P_{max} is the peak stress, ω is the frequency of the dynamic load.

According to the test data, the incident stress wave was simulated. The simulating result is shown in the Fig. 6. The half-sine stress wave with the amplitude of 215 MPa and the delay of 200 μ s is in agreement with the measured value. During the simulation, samples with different freeze-thaw cycles could reach to the same strain rate through changing the amplitude of the half-sine wave (This is equivalent to change the bullet's initial speed in the laboratory test).

3.2 Parameters of HJC Constitutive Model

The HJC model could be used to simulate the large deformation mechanical behavior of rock under the high strain rate. It has been introduced by LS-DYNA procedure, and widely applied in the numerical simulation.

There are three parts in the HJC model, including: equation of state, strength mode, and damage model (Holmquist et al. 1993). There are 21 material parameters in the HJC model, that are, density ρ_0 ; static compressive strength f_c ; strength parameters: A, B, N, C, SMAX, G; damage parameters: D_1 , D_2 , EFMIN; pressure parameters: P_c , μ_c , K_1 , K_2 , K_3 , P_1 , μ_1 , T; software parameters: $\dot{\epsilon}$, f_s .

The calculation model with the static compressive strength of 48 MPa, tensile strength of 4 MPa, and the density of 2410 kg/m³ for the concrete was given by Holmquist et al. (1993), seen in Table 2.

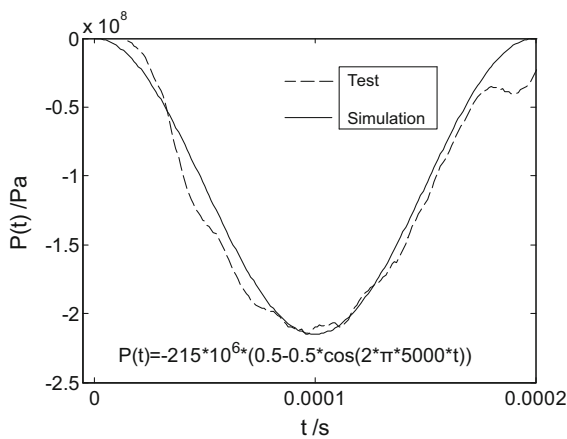


Fig. 6 Testing and simulation curve of the incident wave

The sensitivity and selection methods of these 21 parameters have been systematically studied (Wen et al. 2016). Part of granite parameters under different freeze-thaw cycles could be determined based on the Table 2. SMAX and D_2 could be selected according to the initial parameters. Parameters K_1 , K_2 , K_3 , P_1 , μ_1 could be selected according to the Hugoniot relationship of the impact compression empirical constants (Christopher 2011). Parameter C could be obtained from the relationship between the equivalent stress σ^* and logarithmic strain rate, and parameter A could be calculated from the Eq. (2).

$$\frac{A - 0.75}{\ln 10^0 - \ln 10^{-4}} = C \tag{2}$$

The shear modulus G, bulk modulus K of the rock could be determined by Eqs. (3) and (4).

$$G = \frac{E}{2(1 + \nu)} \tag{3}$$

$$K = \frac{E}{3(1 - 2\nu)} \tag{4}$$

where G is the shear modulus; K is the bulk modulus; E is the elasticity modulus; ν is the Poisson's ratio.

P_c could be calculated used the formula (Holmquist et al. 1993), that is, $P_c = f_c/3$.

Because $P_c = K\mu_c$, therefore,

$$\mu_c = \frac{P_c}{K} = \frac{f_c(1 - 2\nu)}{E} \tag{5}$$

D_1 could be determined using Eq. (6).

$$D_1 = 0.01/(1/6 + T^*) \tag{6}$$

It could use the above-mentioned ANSYS calculation model to select B and N, and use the formula (7) (Li 2014) to obtain the dynamic stress–strain curve. The simulating stress–strain curve could be close to the measured value through adjustment of B and N. The peak stress of the stress–strain curve increases with the increase of B, while the peak strain remains constant. N has great impact on the shape of the yield stage of the curve. The selected parameters of HJC constitutive model are shown in Table 3.

$$\begin{aligned} \epsilon(t) &= -\frac{2C_0}{l_s} \int_0^t \epsilon_r(t) dt, \quad \sigma(t) = \frac{A_0}{A_s} E_0 \epsilon_r(t), \quad \dot{\epsilon}(t) \\ &= -\frac{2C_0}{l_s} \dot{\epsilon}_r(t) \end{aligned} \tag{7}$$

Table 2 Initial parameters of HJC model

$\rho_0/\text{kg/m}^3$	f_c/MPa	A	B	N	C	SMAX	G/GPa	D_1	D_2	EFMIN
2595	80.27	0.79	1.6	0.61	0.007	7.0	15.6	0.037	1.0	0.01
P_c/MPa	μ_c	K_1/GPa	K_2/GPa	K_3/GPa	P_1/GPa	μ_1	T/MPa	$\dot{\epsilon}$	f_s	
26.76	$1.01e - 3$	85	- 171	208	1.0	0.100	8.42	$1e - 6$	0.004	

Table 3 Parameters of HJC constitutive model

Parameter	0 cycles	20 cycles	40 cycles	60 cycles
$\rho_0/\text{kg/m}^3$	2727.5	2725.4	2722.3	2721.9
f_c/MPa	117.2	106.7	84.5	72.0
A	0.759	0.757	0.759	0.757
B	1.12	0.94	0.83	0.82
C	0.0010	0.0008	0.0010	0.0008
N	1.30	1.25	1.15	1.22
SMAX	7.0	7.0	7.0	7.0
G/GPa	10.15	7.15	5.36	4.01
D_1	0.041	0.042	0.042	0.042
D_2	1.0	1.0	1.0	1.0
EFMIN	0.01	0.01	0.01	0.01
P_c/MPa	39.1	35.6	28.2	24.0
μ_c	2.23×10^{-3}	2.81×10^{-3}	2.89×10^{-3}	3.33×10^{-3}
P_1/GPa	1.4	1.2	1.2	1.1
μ_1	0.100	0.101	0.101	0.101
K_1/GPa	12	12	12	12
K_2/GPa	25	25	25	25
K_3/GPa	42	42	42	42
T/MPa	8.77	7.56	5.84	5.22
$\dot{\epsilon}$	1×10^{-6}	1×10^{-6}	1×10^{-6}	1×10^{-6}
f_s	0.004	0.004	0.004	0.004

where E_0, C_0, A_0 are the elastic modulus, elastic wave velocity and cross-sectional area of the bar, respectively. A_s, l_s are the initial cross-sectional area and the length of sample, respectively.

The comparison of the simulation curves used the HJC model by LS-DYNA and the measured curves obtained by SHPB test are shown in Fig. 7. The simulation values are in good agreement with the measured values, indicating the parameters of the HJC model are reliable.

From Fig. 7, the stress–strain simulation curves and measured curves are in good agreement before the peak value, indicating the simulation results are reliable for analyzing the strength of the rock. The

dynamic stress–strain curves obtained by numerical simulation and tests after the peak are different, it is because the numerical simulation could not fully simulate the rock fracture. The study focus on the peak and pre-peak of the stress–strain curve, and the difference of the curves after the peak doesn't infect the results.

4 Analysis of Dynamic Strength

Through changing the amplitude of the incident wave to adjust the strain rate of samples in the numerical simulations, the strain rate of the samples could reach the same value under different freeze-thaw cycles.

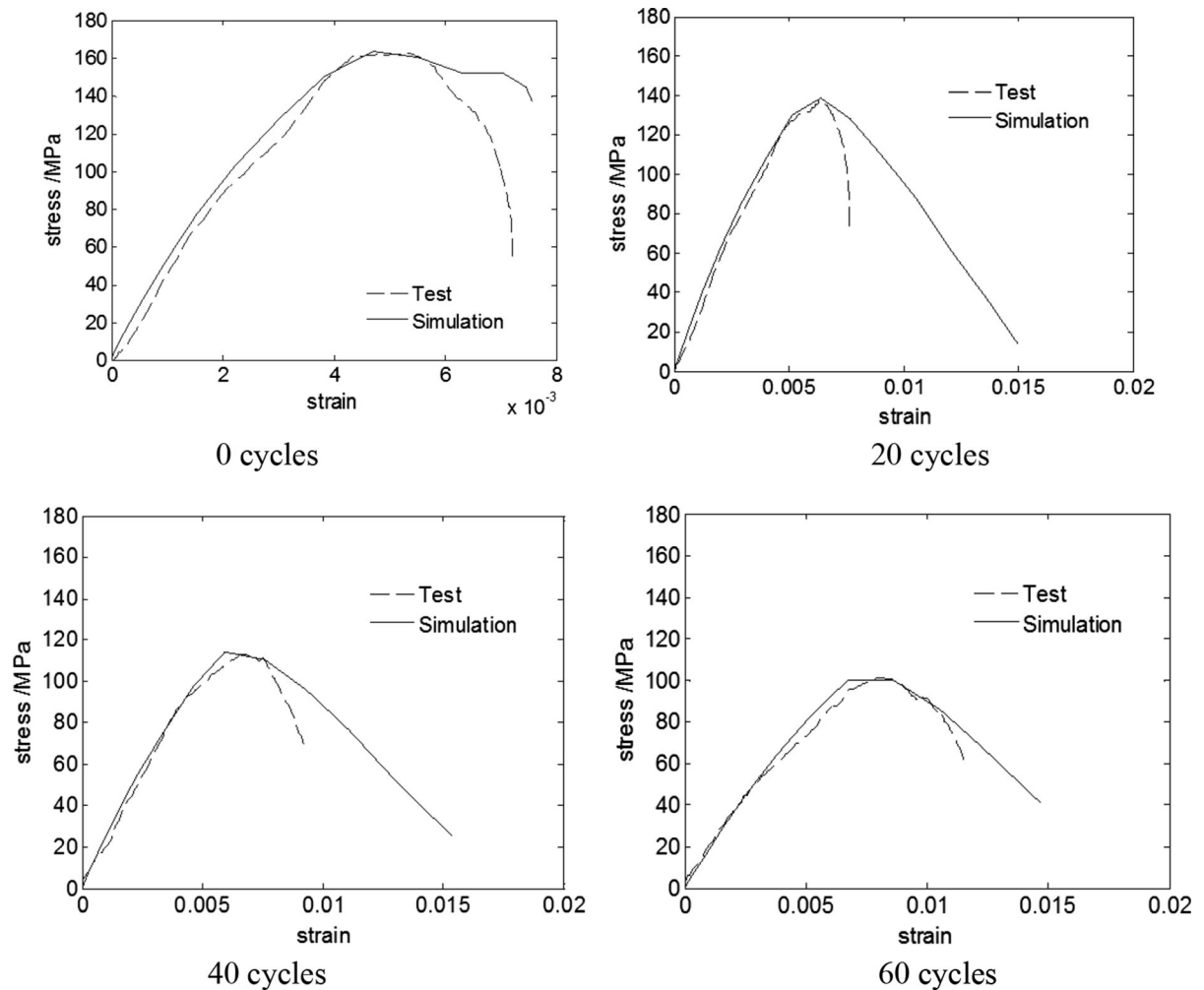


Fig. 7 Comparison between stress–strain simulation curves and measured curve

Combined the laboratory testing results with the numerical simulation results obtained by the LS-DYNA numerical simulation used HJC constitutive model (Parameters of HJC shown in Table 3), the statistical table between the dynamic strength with the

Table 4 Statistical table between dynamics strength with strain rate and freeze-thaw cycles (unit: MPa)

Strain rate	0 cycles	20 cycles	40 cycles	60 cycles
76.4	150.2	141.5	117.9	107.8
100.1	161.0	156.9	125.55	112.6
130.2	176.1	167.4	138.6	127.6

strain rate and the freeze-thaw cycles for the granite samples were obtained, shown in Table 4.

The dynamic strength of the granite samples have the strain rate effects both under the normal temperature and the freeze-thaw cycles. Under the same freeze-thaw cycles, the dynamic strength of the granite increases with increase of the strain rate, which could be simulated used the exponential function, shown in Eq. (8) [the parameters a and b in Eq. (8) are shown in the Table 5, the simulating curve is shown in Fig. 8. Many scholars Lajtai et al. 1991; Li 2014; Li et al. 2005] have obtained the change law of the increase of the dynamic strength with the strain rate for the rock under the normal temperature. The important parameter b in Eq. (8) is approximately equal to 0.3 (Li et al.

Table 5 Parameters a and b of the Eq. (8) and R-square of the curve-fitting

Freeze-thaw cycles	a	b	R ²
0	40.60	0.301	0.99
20	36.88	0.311	0.98
40	30.92	0.307	0.98
60	25.97	0.325	0.93

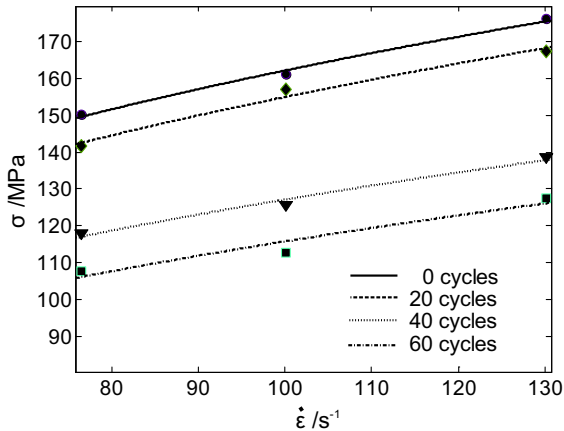


Fig. 8 Relationship between dynamic strength and strain rate of granite samples under the same freeze-thaw cycles

1994; Cusatis 2011; Lajtai et al. 1991), which is similar to the results of this study.

$$\sigma = a\dot{\epsilon}^b \tag{8}$$

Under the same strain rate, the dynamic strength of the granite decreases gradually with increase of the freeze-thaw cycles. The tool box of Matlab for curve simulation is used to simulate the relationship between the dynamic strength and freeze-thaw cycles under the same strain rate. SHPB is a instrument for studying the dynamic mechanical properties of rock samples under intermediate strain rate. The strain rate is 76.4 s⁻¹, 100.1 s⁻¹ and 130.2 s⁻¹ respectively, which are determined by the tests and numerical simulation results, and the interval between the three strain rates is moderate. The simulation curve is shown in Fig. 9, and the simulation formula is shown in Eq. (9). The parameters α and β of Eq. (9) are shown in Table 6. The parameter α is approximately equal to the initial strength of the granite; the parameter β reflects the strength degradation of the granite with freeze-

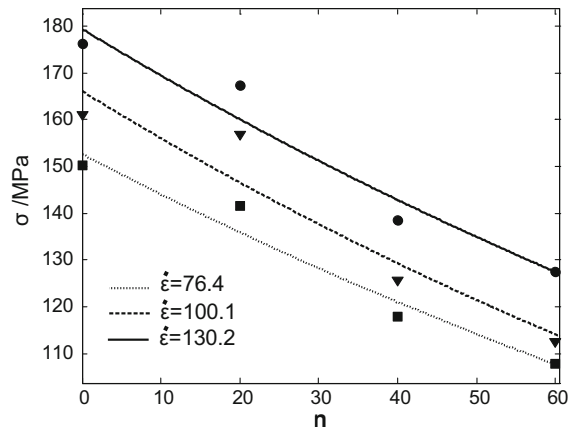


Fig. 9 Relationship between dynamic strength and cycle times under the same strain rate

Table 6 The parameters α and β of the formula (9) and R-square of the curve-fitting

$\dot{\epsilon}$	α	β	R ²
76.4	152.7	- 0.0058	0.96
100.1	166.1	- 0.0063	0.91
130.2	179.3	- 0.0057	0.95

thaw cycles, and β is negative, represents the dynamic intensity decreases with the increase of freeze-thaw cycles, and the greater of the absolute value of β indicates a faster reduction in strength.

$$\sigma = \alpha \cdot e^{\beta n} \tag{9}$$

This paper provides a new method of studying strength of rock under coupled dynamic loads and freeze-thaw cycles. The development of the interior micro crack of rock is caused by the freeze-thaw cycles, so the interior micro crack became more developed and dynamic strength became more smaller with more freeze-thaw cycles. The dynamic strength increases with the increase of the strain rate, but the increase rate is weakened gradually due to the effect of freeze-thaw deterioration. The dynamic strength is associated with the strain rate and the freeze-thaw cycles, but their influential effects are opposite and interconnection.

5 Conclusions

- There is no compaction stage in the stress–strain curve under the impact load for the rock sample. The shapes of the curves before and after the freeze-thaw are different, mainly reflected in the peak stress and the slope of elastic stage of the stress–strain curve.
- The dynamic strength of granite has the strain rate effect both under the normal temperature and the freeze-thaw cycles. Under the same freeze-thaw cycles, the dynamic strength of granite increases with the increase of the strain rate, which could be simulated used the exponential function ($\sigma = a\varepsilon^b$). The parameter b in the exponential function is approximately equal to 0.3.
- Under the same strain rate, the dynamic strength of the granite gradually decreases with the increase of the freeze-thaw cycles. The relationship between the dynamic strength and the freeze-thaw cycles could be expressed used the index function ($\sigma = \alpha \cdot e^{\beta n}$). The parameter α is approximately equal to initial strength of the rock, and the parameter β reflects the strength degradation of the rock with freeze-thaw cycles.
- The dynamic strength of granite is associated with the strain rate and the freeze-thaw cycles, but the influential effects are interconnected and opposite.

Acknowledgements We are grateful to the Fund of Natural science foundation of Hebei Province (E2018210066) and China Postdoctoral Science Foundation (2018M631758) for the continuing support of our work. The authors are deeply grateful for this financial support.

References

- Altindag R, Alyildiz IS, Onargan T (2004) Mechanical property degradation of ignimbrite subjected to recurrent freeze-thaw cycles. *Int J Rock Mech Min Sci* 41:1023–1028
- Amin J, Nikudel MR, Khamchian M (2013) Predicting the long-term durability of building stones against freeze-thaw using a decay function model. *Cold Reg Sci Technol* 92:29–36. <https://doi.org/10.1016/j.coldregions.2013.03.007>
- Anderson CE Jr, O'donoghue PE (1992) Numerical simulations of SHPB experiments for the dynamic compressive strength and failure of ceramics. *Int J Fracture* 55:193–208
- Bailly P, Delvare F, Vial J, Hanus JL, Biessy M, Picart D (2011) Dynamic behavior of an aggregate material at simultaneous high pressure and strain rate: SHPB triaxial tests. *Int J Impact Eng* 38:73–84. <https://doi.org/10.1016/j.ijimpeng.2010.10.005>
- Bell FG (2000) Engineering properties of soils and rocks, 4th edn. Blackwell Science, Hoboken
- Celik MY (2017) Water absorption and P-wave velocity changes during freeze-thaw weathering process of crosscut travertine rocks. *Environ Earth Sci* 76(12):409
- Christopher SM (2011) Development of geomaterial parameters for numerical simulations using the Holmquist–Johnson–Cook constitutive model for concrete. ARL-TR-5556, U.S. Army Research Laboratory, Orlando
- Cusatis G (2011) Strain-rate effects on concrete behavior. *Int J Impact Eng* 38:162–170
- Dong G (2005) The numerical simulation of split Hopkinson pressure bar experimental technique. HeFei University of Technology, Hefei
- Ghobadi MH, Beydokhti ART, Nikudel MR (2016) The effect of freeze-thaw process on the physical and mechanical properties of tuff. *Environ Earth Sci* 75(9):846. <https://doi.org/10.1007/s12665-016-5664-8>
- Graham J, Au VCS (1985) Effects of freeze-thaw and softening on natural clay at low stresses. *Can Geotech J* 22:69–78
- Hashemi M, Goudarzi MB, Jamshidi A (2018) Experimental investigation on the performance of Schmidt hammer test in durability assessment of carbonate building stones against freeze-thaw weathering. *Environ Earth Sci* 77:684
- Holmquist TJ, Johnson GR, Cook WH (1993) “A computational constitutive model for concrete subjective to large strains, high strain rates and high pressures”. presented at International Symposium on Ballistics 14, pp 591–600
- Huang S, Liu Q, Cheng A, Liu Y (2018) A statistical damage constitutive model under freeze-thaw and loading for rock and its engineering application. *Cold Reg Sci Technol* 145:142–150. <https://doi.org/10.1016/j.coldregions.2017.10.015>
- Ince I, Fener M (2016) A prediction model for uniaxial compressive strength of deteriorated pyroclastic rocks due to freeze-thaw cycle. *J Afr Earth Sci* 120:134–140. <https://doi.org/10.1016/j.jafrearsci.2016.05.001>
- Khoogar AR, Mohades MA, Vahedi Kh (2013) A novel study of penetration into concrete targets by ogive nose projectiles. *Int J Adv Des Manuf Technol* 6(3):1–7
- Khuda S, Albermani F, Veidt M (2017) Flexural strength of weathered granites: Influence of freeze and thaw cycles. *Constr Build Mater* 156:891–901. <https://doi.org/10.1016/j.conbuildmat.2017.09.049>
- Lajtai EZ, Scott Duncan EJ, Carter BJ (1991) The effect of strain rate on rock strength. *Rock Mech Rock Eng* 24(2):99–109
- Li X (2014) Rock dynamics fundamentals and applications. Science Press, Beijing
- Li X, Chen S, Gu D (1994) Dynamic strength of rock under impulse loads with different stress waveforms and durations. *J Cent-South Inst Min Metall* 25(3):30
- Li XB, Lok TS, Zhao J (2005) Dynamic characteristics of granite subjected to intermediate loading rate. *Rock Mech Rock Eng* 38(1):21–39
- Li JL, Zhou KP, Liu WJ, Deng HW (2016) NMR research on deterioration characteristics of microscopic structure of sandstones in freeze-thaw cycles. *Trans Nonferrous Met*

- Soc China 26(11):2997–3003. [https://doi.org/10.1016/S1003-6326\(16\)64430-8](https://doi.org/10.1016/S1003-6326(16)64430-8)
- Liping W, Ning L, Jilin Q, Yanzhe T, Shuanhai X (2019) A study on the physical index change and triaxial compression test of intact hard rock subjected to freeze-thaw cycles. *Cold Reg Sci Technol* 160:39–47
- Liu F, Chen G, Li L, Guo Y (2012) Study of impact performance of rubber reinforced concrete. *Constr Build Mater* 36:604–616
- Liu H, Yang G, Ye W (2016) Analysis of water and ice content and damage characteristics of the frozen rock during freezing based on the three-valued segmentation of CT images. *J Min Saf Eng* 33(6):1130–1137
- Mutluturk M, Altindag R, Turk G (2004) “A decay function model for the integrity loss of rock when subjected to recurrent cycles of freezing-thawing and heating-cooling”. *Int J Rock Mech Min Sci* 41:237–244
- Polanco-Loria M, Hopperstad OS, Borvik T, Berstad T (2008) Numerical predictions of ballistic limits for concrete slabs using a modified version of the HJC concrete model. *Int J Impact Eng* 35:290–303. <https://doi.org/10.1016/j.ijimpeng.2007.03.001>
- Saad A, Guedon S, Martineau F (2010) Microstructural weathering of sedimentary rocks by freeze-thaw cycles: experimental study of state and transfer parameters. *Comptes Rendus Geosci* 342:197–203. <https://doi.org/10.1016/j.crte.2009.12.009>
- SL264-2001 (2001) Specifications for rock tests in water conservancy and hydroelectric engineering. Yangtze River Scientific Research Institute, Wuhan
- Sondergeld CH, Rai CS (2007) Velocity and resistivity changes during freeze-thaw cycles in Berea sandstone. *Geophysics* 72(2):99–105. <https://doi.org/10.1190/1.2435198>
- Walbert C, Eslami J, Beaucour AL (2015) Evolution of the mechanical behaviour of limestone subjected to freeze-thaw cycles. *Environ Earth Sci* 74(7):6339–6351. <https://doi.org/10.1007/s12665-015-4658-2>
- Wen L, Li X, Wu Q (2016) Study on parameters of Holmquist–Johnson–Cook model for granite porphyry. *Chin J Comput Mech* 33(5):725–731
- Wu X, Li Y, Li H (2011) Research on the material constants of the HJC dynamic constitutive model for concrete. *Chin J Appl Mech* 25(1):15–22
- Xu G (2006) Study on mechanical characteristics of rock at low temperature, damage due to freezing and thawing and mutiphysical coupling problems of rock in cold regions. Graduate University of the Chinese Academy of Sciences, Beijing
- Yavuz H, Altindag R, Sarac S, Ugur I, Sengun N (2006) Estimating the index properties of deteriorated carbonate rocks due to freeze-thaw and thermal shock weathering. *Int J Rock Mech Min Sci* 43:767–775. <https://doi.org/10.1016/j.ijrmms.2005.12.004>
- Yu M, Zha X, Ye J (2010) The influence of joints and composite floor slabs on effective tying of steel structures in preventing progressive collapse. *J Constr Steel Res* 66(3):442–451. <https://doi.org/10.1016/j.jcsr.2009.10.008>

Publisher’s Note Springer Nature remains neutral with regard to jurisdictional claims in published maps and institutional affiliations.